
# Target Material Activation Calculations for High Gain Light Ion Fusion Targets

D.L. Henderson, A.M. White and G.A. Moses

April 1984
(revised May 1987)

UWFDM-572

FUSION TECHNOLOGY INSTITUTE

UNIVERSITY OF WISCONSIN

MADISON WISCONSIN

# Target Material Activation Calculations for High Gain Light Ion Fusion Targets

D.L. Henderson, A.M. White and G.A. Moses

Fusion Technology Institute
University of Wisconsin
1500 Engineering Drive
Madison, WI 53706

http://fti.neep.wisc.edu

April 1984 (revised May 1987)

UWFDM-572

# TARGET MATERIAL ACTIVATION CALCULATIONS FOR HIGH GAIN LIGHT ION FUSION TARGETS

D.L. Henderson

A.M. White

G.A. Moses

Fusion Engineering Program
Nuclear Engineering Department
University of Wisconsin-Madison
Madison, Wisconsin 53706

April 1984

(Revised August 1985)

(Revised May 1987)

UWFDM-572

Abstract

Radioactivity calculations were performed on several light ion driven targets with different tamper and pusher/ablator materials to determine the magnitude of the neutron induced radioactivity. The materials examined were $CH_2$, LiPb and BeO as pusher/ablator materials and W, Pb and Au as tamper materials. A 1 mg DT fuel load and a 30% fuel burnup were assumed for the calculations. The initial activity levels for the targets are due to the pusher/ablator materials which produce the isotope $^{6}_{2}He$ ($t_{1/2}$ = 810 ms). Activity levels for times greater than 1 minute were on the order of 0.3 to 2 curies depending on the tamper material.

## 1. Introduction

The light ion beam fusion target development facility (TDF) is an experimental facility designed to verify the feasibility of using the light ion beam pulsed power technology to initiate thermonuclear burn in small specially designed high gain ICF targets. Activation of the target and reactor chamber structural materials occurs as the high energy neutrons released by the initiation and subsequent burn of the DT fuel interact with the materials. Since this is a development facility, easy access to the reactor chamber and to its interior is of importance, hence one would like to keep the induced radioactivity at a minimum.

Several first wall materials were surveyed as possible candidates for the TDF design and the results were presented at the Fifth ANS Topical Meeting on the Technology of Fusion Energy.[1] The first wall material examined and shown to have the lowest dose rate after a 1 week shutdown period was Al-6061. The activation of the target material, however, was not examined in Ref. 1. This subject is treated in the present paper.

## 2. Calculational Model

### 2.1 Target Calculation

The target analyzed in this paper (Fig. 1) was originally published by Bangerter and Meeker[2] and a modified version of it was presented by the University of Wisconsin in the HIBALL Heavy Ion Beam Fusion Reactor Design Study.[3] Further calculations performed by Long and Tahir[4] showed that the tamper density decreased to 10% of its initial value due to heating by the impinging ion beams. A tamper density of 10% natural density was chosen to be representative of this ion beam heating.

Four different target material combinations were examined and are given in Table 1. For all cases, the target DT load was assumed to be 1 mg and the fuel was assumed to be compressed to a density times radius product ($\rho R$ value) of 2.0 g/cm$^2$. A 30% fuel burnup fraction was assumed, giving approximately 100 MJ of released fusion energy (71 MJ of released neutron energy).

One neutron transport calculation was performed using the Case I material composition (see Table 2) and the target configuration depicted in Fig. 2. The scalar flux values computed were used as input for the 4 different target activation analysis cases. The justification for performing only one neutron transport calculation is that previous target analysis calculations[2,5] have shown that the neutron leakage spectrum for targets of the type examined in this paper is primarily determined by the neutron moderation within the DT fuel region. Thus very little additional moderation takes place within the outer surrounding regions. The amount of neutron moderation taking place within the target is shown in Fig. 3. The peak around 14.1 MeV is due to uncollided neutrons escaping the target. The two lower peaks are due to neutron scattering off of deuterium and tritium and are related to the "Placzek wiggles" which were obtained by Placzek in his classical neutron slowing down work.[6,7] Also of some importance are the secondary neutrons released by (n,2n) reactions contributing to the leakage spectrum from approximately 8 MeV on downward. Additional details on the characteristics of the spectrum and corresponding target configuration can be found in Ref. 3.

There is one case presented (which will be noted) that uses a 14.1 MeV monoenergetic neutron source applied to the inner surface of Region 2 (see Fig. 2). This allowed a comparison of the activity resulting from a moderated target spectrum and 14.1 MeV monoenergetic neutron source.

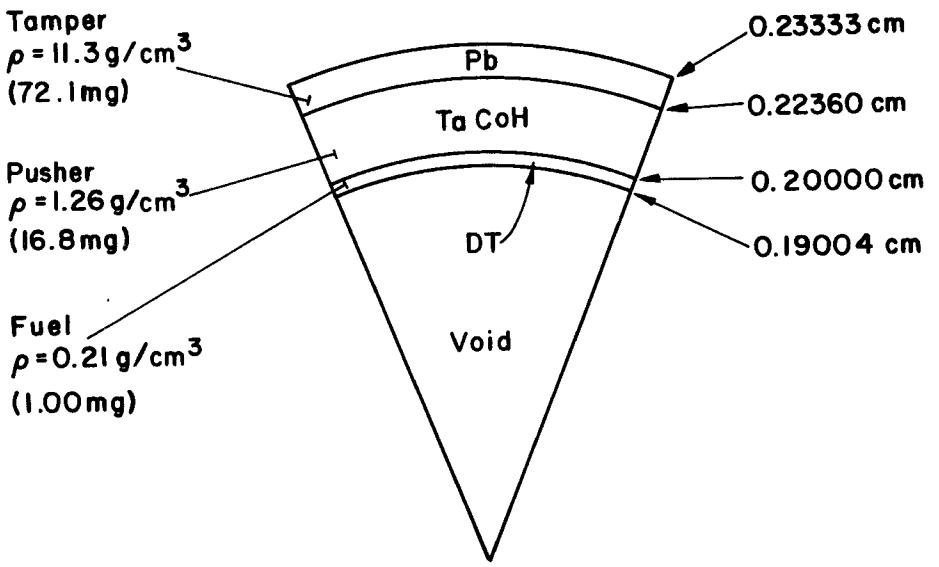


Fig. 1. Ion beam fusion target as depicted by R.O. Bangerter in Ref. 2.

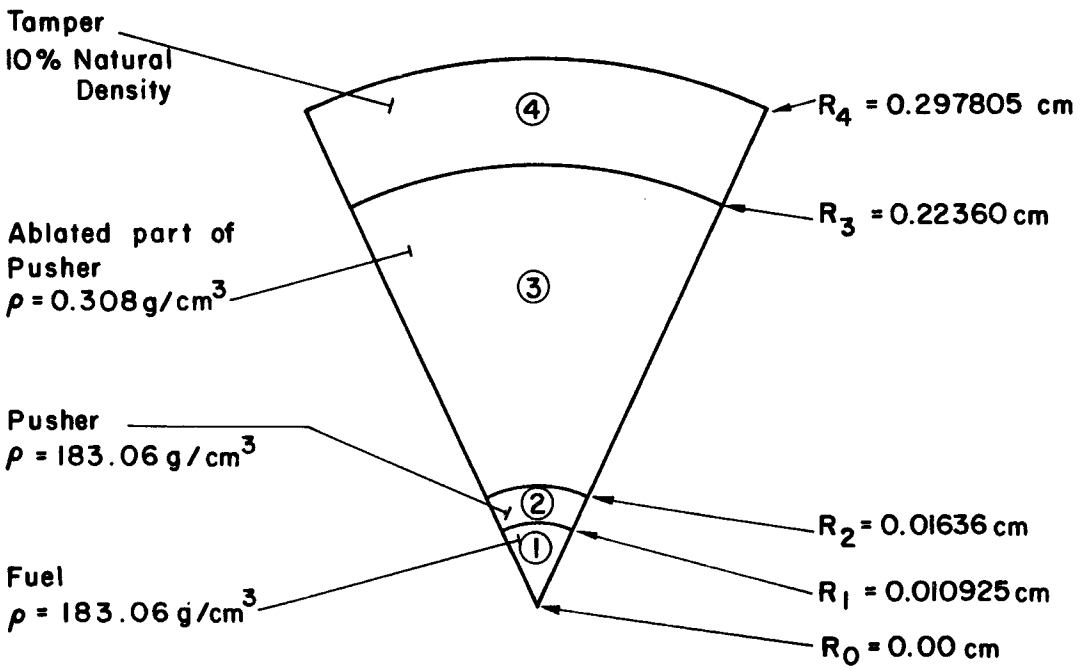


Fig. 2. The compressed target configuration used with the Case I material composition for the neutronic and radioactivity calculations.

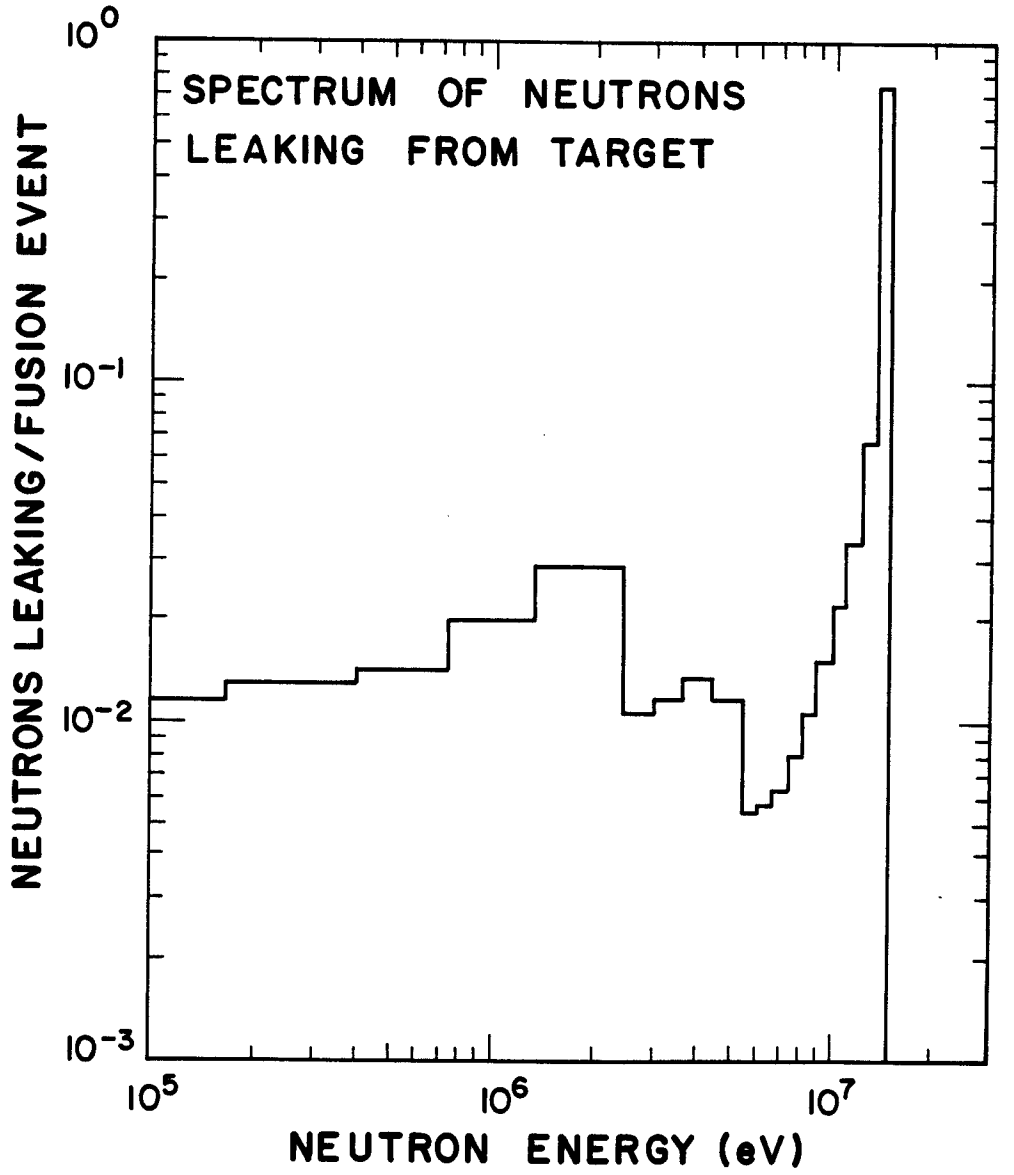


Fig. 3. The spectrum of neutrons leaking from the ion beam target normalized to one fusion neutron.

TABLE 1. TARGET MATERIALS USED IN ACTIVATION CALCULATIONS

| | Case I | | Case II | | Case III | | Case IV | |
|---|---|---|---|---|---|---|---|---|
| Region | Comp. | Mass | Comp. | Mass | Comp. | Mass | Comp. | Mass |
| 1 | DT | 1 mg | DT | 1 mg | DT | 1 mg | DT | 1 mg |
| 2 | LiPb | 2.36 mg | $CH_2$ | 2.36 mg | $CH_2$ | 2.36 mg | BeO | 2.36 mg |
| 3 | LiPb | 14.42 mg | $CH_2$ | 14.42 mg | $CH_2$ | 14.42 mg | BeO | 14.42 mg |
| 4 | Pb | 72.13 mg | W | 122.55 mg | Au | 123.32 mg | W | 122.55 mg |

## 2.2 Activation Calculations

The scalar fluxes obtained from the target neutronic calculations were used to compute neutron transmutations and these in turn served as source terms within the radioactivity decay equations

$$\frac{dN_i}{dt} = S_i - \lambda_i N_i - \sum_{i \to y} \phi \qquad \text{where } S_i = \sum_{x \to i} \phi \, . \tag{1}$$

The production of each isotope, its subsequent decay and possible decay chaining is computed by the DKR code.[8] Table 2 contains the atomic densities of the original isotopes for each case. The decay chains examined by the DKR code for the different isotopes considered are given in Table 3. Here the nuclear reaction is denoted by the usual notation. The decay mode and half-life are also given.

## 2.3 Codes and Data Libraries

The one-dimensional discrete ordinates code ANISN[9] was used to obtain the neutron scalar flux distribution throughout the different regions of the target. The main options used in the calculation are given below.

TABLE 2. ISOTOPIC DENSITIES OF TARGET MATERIALS

| Region | Case I | | Case II | | Case III | | Case IV | |
|---|---|---|---|---|---|---|---|---|
| | Isotope | Density [atoms/b-cm] | Isotope | Density [atoms/b-cm] | Isotope | Density [atoms/b-cm] | Isotope | Density [atoms/b-cm] |
| 1 | D | 22.225 | D | 22.225 | D | 22.225 | D | 22.225 |
| | T | 22.225 | T | 22.225 | T | 22.225 | T | 22.225 |
| 2 | $^{6}Li$ | 4.656-1 | C | 7.860 | C | 7.860 | Be | 4.409 |
| | $^{7}Li$ | 5.809 | H | 15.720 | H | 15.720 | $^{16}O$ | 4.398 |
| | $^{204}Pb$ | 4.616-3 | | | | | $^{17}O$ | 1.675-3 |
| | $^{206}Pb$ | 7.835-2 | | | | | $^{18}O$ | 8.993-3 |
| | $^{207}Pb$ | 7.184-2 | | | | | | |
| | $^{208}Pb$ | 1.704-1 | | | | | | |
| 3 | $^{6}Li$ | 7.834-4 | C | 1.322-2 | C | 1.322-2 | Be | 7.417-3 |
| | $^{7}Li$ | 9.774-3 | H | 2.644-2 | H | 2.644-2 | $^{16}O$ | 7.399-3 |
| | $^{204}Pb$ | 7.767-6 | | | | | $^{17}O$ | 2.819-6 |
| | $^{206}Pb$ | 1.318-4 | | | | | $^{18}O$ | 1.513-5 |
| | $^{207}Pb$ | 1.209-4 | | | | | | |
| | $^{208}Pb$ | 2.866-4 | | | | | | |
| 4 | $^{204}Pb$ | 4.663-5 | $^{180}W$ | 8.177-6 | $^{197}Au$ | 5.908-3 | $^{180}W$ | 8.177-6 |
| | $^{206}Pb$ | 7.914-4 | $^{182}W$ | 1.654-3 | | | $^{182}W$ | 1.654-3 |
| | $^{207}Pb$ | 7.257-4 | $^{183}W$ | 8.994-4 | | | $^{183}W$ | 8.944-4 |
| | $^{208}Pb$ | 1.721-3 | $^{184}W$ | 1.929-3 | | | $^{184}W$ | 1.929-3 |
| | | | $^{186}W$ | 1.799-3 | | | $^{186}W$ | 1.799-3 |

## TABLE 3. NUCLEAR DECAY CHAINS USED BY DKR

| | | |
|---|---|---|
| isotope | $^{6}_{3}Li \rightarrow (n,p)\ ^{6}_{2}He$ | decays by $\beta^-$, $t_{1/2} = 0.810$ sec $\rightarrow\ ^{6}_{3}Li$ |
| isotope | $^{7}_{3}Li \rightarrow \begin{matrix}(n,d)\\(n,n')p\end{matrix}\ ^{6}_{2}He$ | decays by $\beta^-$, $t_{1/2} = 0.810$ sec $\rightarrow\ ^{6}_{3}Li$ |
| | $^{7}_{3}Li \rightarrow (n,\gamma)\ ^{8}_{3}Li$ | decays by $\beta^-$, $t_{1/2} = 0.842$ sec $\rightarrow\ ^{8}_{4}Be$ |
| | | $^{8}_{4}Be \rightarrow 2\ ^{4}_{2}He$, $t_{1/2} \sim 2 \times 10^{-16}$ sec |
| isotope | $^{9}_{4}Be \rightarrow (n,\alpha)\ ^{6}_{2}He$ | decays by $\beta^-$, $t_{1/2} = 0.810$ sec $\rightarrow\ ^{6}_{3}Li$ |
| | $^{9}_{4}Be \rightarrow (n,p)\ ^{9}_{3}Li$ | decays by $\beta^-$, $t_{1/2} = 0.178$ sec $\rightarrow\ ^{9}_{4}Be$ |
| | $^{9}_{4}Be \rightarrow (n,\gamma)\ ^{10}_{4}Be$ | decays by $\beta^-$, $t_{1/2} = 1.6 \times 10^{6}$ yrs $\rightarrow\ ^{10}_{5}B$ |
| isotope | $^{12}_{6}C \rightarrow (n,\alpha)\ ^{9}_{4}Be \rightarrow (n,p)\ ^{9}_{3}Li$ | decays by $\beta^-$, $t_{1/2} = 0.178$ sec $\rightarrow\ ^{9}_{4}Be$ |
| | $^{12}_{6}C \rightarrow (n,\alpha)\ ^{9}_{4}Be \rightarrow (n,\gamma)\ ^{10}_{4}Be$ | decays by $\beta^-$, $t_{1/2} = 1.6 \times 10^{6}$ yrs $\rightarrow\ ^{10}_{5}B$ |
| | $^{12}_{6}C \rightarrow (n,\alpha)\ ^{9}_{4}Be \rightarrow (n,\alpha)\ ^{6}_{2}He$ | decays by $\beta^-$, $t_{1/2} = 0.810$ sec $\rightarrow\ ^{6}_{3}Li$ |
| isotope | $^{13}_{6}C \rightarrow (n,\gamma)\ ^{14}_{6}C$ | decays by $\beta^-$, $t_{1/2} = 5734$ yrs $\rightarrow\ ^{14}_{7}N$ |
| isotope | $^{16}_{8}O \rightarrow (n,p)\ ^{16}_{7}N$ | decays by $\beta^-$, $t_{1/2} = 7.10$ sec $\rightarrow\ ^{16}_{8}O$ |
| | $^{16}_{8}O \rightarrow (n,\alpha)\ ^{13}_{6}C \rightarrow\ ^{13}_{6}C(n,\gamma)\ ^{14}_{6}C$ | decays by $\beta^-$, $t_{1/2} = 5734$ yrs $\rightarrow\ ^{14}_{7}N$ |
| isotope | $^{182}_{74}W \rightarrow (n,p)\ ^{182}_{73}Ta$ | decays by $\beta^-$, $t_{1/2} = 115$ days $\rightarrow\ ^{182}_{74}W$ |
| | $^{182}_{74}W \rightarrow (n,2n)\ ^{181}_{74}W$ | decays by EC, $t_{1/2} = 121$ days $\rightarrow\ ^{181}_{73}Ta$ |
| | $^{182}_{74}W \rightarrow (n,\gamma)\ ^{183}_{74}W \rightarrow (n,n')p\ ^{182}_{73}Ta$ | decays by $\beta^-$, $t_{1/2} = 115$ days $\rightarrow\ ^{182}_{74}W$ |
| | $^{182}_{74}W \rightarrow (n,\gamma)\ ^{183}_{74}W \rightarrow (n,p)\ ^{183}_{73}Ta$ | decays by $\beta^-$, $t_{1/2} = 5.0$ days $\rightarrow\ ^{183}_{74}W$ |

| | | | |
|---|---|---|---|
| isotope | $^{183}_{74}W \rightarrow$ (n,d) or (n,n')p $^{182}_{73}Ta$ | decays by $\beta^-$, $t_{1/2}$ = 115 days → | $^{182}_{74}W$ |
| | $^{183}_{74}W \rightarrow$ (n,p) $^{183}_{73}Ta$ | decays by $\beta^-$, $t_{1/2}$ = 5.0 days → | $^{183}_{74}W$ |
| | $^{183}_{74}W \rightarrow$ (n,2n) $^{182}_{74}W \rightarrow$ (n,p) $^{182}_{73}Ta$ | decays by $\beta^-$, $t_{1/2}$ = 115 days → | $^{182}_{74}W$ |
| | $^{183}_{74}W \rightarrow$ (n,2n) $^{182}_{74}W \rightarrow$ (n,2n) $^{181}_{74}W$ | decays by EC, $t_{1/2}$ = 121 days → | $^{181}_{73}Ta$ |
| | $^{183}_{74}W \rightarrow$ (n,$\gamma$) $^{184}_{74}W \rightarrow$ (n,$\alpha$) $^{181}_{72}Hf$ | decays by $\beta^-$, $t_{1/2}$ = 42.7 days → | $^{181}_{73}Ta$ |
| | $^{183}_{74}W \rightarrow$ (n,$\gamma$) $^{184}_{74}W \rightarrow$ (n,d) or (n,n')p $^{183}_{73}Ta$ | decays by $\beta^-$, $t_{1/2}$ = 5.0 days → | $^{183}_{74}W$ |
| | $^{183}_{74}W \rightarrow$ (n,$\gamma$) $^{184}_{74}W \rightarrow$ (n,p) $^{184}_{73}Ta$ | decays by $\beta^-$, $t_{1/2}$ = 8.7 hrs → | $^{184}_{74}W$ |
| | $^{183}_{74}W \rightarrow$ (n,$\gamma$) $^{184}_{74}W \rightarrow$ (n,$\gamma$) $^{185}_{74}W$ | decays by $\beta^-$, $t_{1/2}$ = 75.1 days → | $^{185}_{75}Re$ |

| | | | |
|---|---|---|---|
| isotope | $^{184}_{74}W \rightarrow$ (n,$\alpha$) $^{181}_{72}Hf$ | decays by $\beta^-$, $t_{1/2}$ = 42.7 days → | $^{181}_{73}Ta$ |
| | $^{184}_{74}W \rightarrow$ (n,d) or (n,n')p $^{183}_{73}Ta$ | decays by $\beta^-$, $t_{1/2}$ = 5.0 days → | $^{183}_{74}W$ |
| | $^{184}_{74}W \rightarrow$ (n,p) $^{184}_{73}Ta$ | decays by $\beta^-$, $t_{1/2}$ = 8.7 hrs → | $^{184}_{74}W$ |
| | $^{184}_{74}W \rightarrow$ (n,$\gamma$) $^{185}_{74}W$ | decays by $\beta^-$, $t_{1/2}$ = 75.1 days → | $^{185}_{75}Re$ |
| | $^{184}_{74}W \rightarrow$ (n,2n) $^{183}_{74}W \rightarrow$ (n,d) or (n,n')p $^{182}_{73}Ta$ | decays by $\beta^-$, $t_{1/2}$ = 115 days → | $^{182}_{74}W$ |
| | $^{184}_{74}W \rightarrow$ (n,2n) $^{183}_{74}W \rightarrow$ (n,p) $^{183}_{73}Ta$ | decays by $\beta^-$, $t_{1/2}$ = 5.0 days → | $^{183}_{74}W$ |

| | | | |
|---|---|---|---|
| isotope | $^{186}_{74}W \rightarrow$ (n,p) $^{186}_{73}Ta$ | decays by $\beta^-$, $t_{1/2}$ = 10.6 min → | $^{186}_{74}W$ |
| | $^{186}_{74}W \rightarrow$ (n,2n) $^{185}_{74}W$ | decays by $\beta^-$, $t_{1/2}$ = 75.1 days → | $^{185}_{75}Re$ |
| | $^{186}_{74}W \rightarrow$ (n,$\gamma$) $^{187}_{74}W$ | decays by $\beta^-$, $t_{1/2}$ = 23.9 hrs → | $^{187}_{75}Re$ |
| | $^{186}_{74}W \rightarrow$ (n,$\alpha$) $^{183}_{72}Hf$ | decays by $\beta^-$, $t_{1/2}$ = 1.06 hrs → | $^{183}_{73}Ta \rightarrow \ldots$ |
| | | ...decays by $\beta^-$, $t_{1/2}$ = 5.0 days → | $^{183}_{74}W$ |
| | $^{186}_{74}W \rightarrow$ (n,d) or (n,n')p $^{185}_{73}Ta$ | decays by $\beta^-$, $t_{1/2}$ = 49.5 min → | $^{185}_{74}W \rightarrow \ldots$ |
| | | ...decays by $\beta^-$, $t_{1/2}$ = 75.1 days → | $^{185}_{75}Re$ |

| | | | |
|---|---|---|---|
| isotope | $^{197}_{79}Au \rightarrow (n,\gamma)\ ^{198}_{79}Au$ | | decays by $\beta^-$, $t_{1/2}$ = 2.67 days $\rightarrow$ $^{198}_{80}Hg$ |
| | $^{197}_{79}Au \rightarrow (n,\alpha)\ ^{194}_{77}Ir$ | | decays by $\beta^-$, $t_{1/2}$ = 19.15 hrs $\rightarrow$ $^{194}_{78}Pt$ |
| | $^{197}_{79}Au \rightarrow (n,2n)\ ^{196}_{79}Au$ | | decays by EC, $t_{1/2}$ = 6.17 days $\rightarrow$ $^{196}_{78}Pt$ |
| | $^{197}_{79}Au \rightarrow (n,2n)\ ^{196}_{79}Au^*$ | | decays by $\gamma$, $t_{1/2}$ = 9.7 hrs $\rightarrow$ $^{196}_{79}Au \rightarrow$... |
| | | | ...decays by EC, $t_{1/2}$ = 6.17 days $\rightarrow$ $^{196}_{78}Pt$ |
| isotope | $^{204}_{82}Pb \rightarrow (n,p)\ ^{204}_{81}Tl$ | | decays by $\beta^-$, $t_{1/2}$ = 3.77 yrs $\rightarrow$ $^{204}_{82}Pb$ |
| | $^{204}_{82}Pb \rightarrow (n,2n)\ ^{203}_{82}Pb$ | | decays by EC, $t_{1/2}$ = 2.17 days $\rightarrow$ $^{203}_{81}Tl$ |
| isotope | $^{206}_{82}Pb \rightarrow (n,\alpha)\ ^{203}_{80}Hg$ | | decays by $\beta^-$, $t_{1/2}$ = 46.64 days $\rightarrow$ $^{203}_{81}Tl$ |
| | $^{206}_{82}Pb \rightarrow (n,t)\ ^{204}_{81}Tl$ | | decays by $\beta^-$, $t_{1/2}$ = 3.77 yrs $\rightarrow$ $^{204}_{82}Pb$ |
| | $^{206}_{82}Pb \rightarrow (n,2n)\ ^{205}_{82}Pb$ | | decays by EC, $t_{1/2}$ = $1.42 \times 10^7$ yrs $\rightarrow$ $^{205}_{81}Tl$ |
| isotope | $^{207}_{82}Pb \rightarrow (n,n)\alpha\ ^{203}_{80}Hg$ | | decays by $\beta^-$, $t_{1/2}$ = 46.64 days $\rightarrow$ $^{203}_{81}Tl$ |
| | $^{207}_{82}Pb \rightarrow (n,2n)\ ^{206}_{82}Pb \rightarrow (n,t)\ ^{204}_{81}Tl$ | | decays by $\beta^-$, $t_{1/2}$ = 3.77 yrs $\rightarrow$ $^{204}_{82}Pb$ |
| | $^{207}_{82}Pb \rightarrow (n,2n)\ ^{206}_{82}Pb \rightarrow (n,2n)\ ^{205}_{82}Pb$ | | decays by EC, $t_{1/2}$ = $1.42 \times 10^7$ yrs $\rightarrow$ $^{205}_{81}Tl$ |
| isotope | $^{208}_{82}Pb \rightarrow (n,\alpha)\ ^{205}_{80}Hg$ | | decays by $\beta^-$, $t_{1/2}$ = 5.49 min $\rightarrow$ $^{205}_{81}Tl$ |
| | $^{208}_{82}Pb \rightarrow (n,\gamma)\ ^{209}_{82}Pb$ | | decays by $\beta^-$, $t_{1/2}$ = 3.28 hrs $\rightarrow$ $^{209}_{83}Bi$ |
| | $^{208}_{82}Pb \rightarrow (n,2n)\ ^{207}_{82}Pb \rightarrow (n,n)\alpha\ ^{203}_{80}Hg$ | | decays by $\beta^-$, $t_{1/2}$ = 46.64 days $\rightarrow$ $^{203}_{81}Tl$ |

- Spherical geometry
- $S_n$ order: $S_4$
- Quadrature set: see Table 4
- Anisotropic scattering option: $P_3$
- Source distribution: uniformly distributed 14.1 MeV monoenergetic source within the fuel region
- Store scalar fluxes: needed for DKR code
- Number of energy groups: 46 groups; 25 neutron and 21 gamma groups
- Number of coarse mesh cells: 4
- Number of fine mesh cells: 39 (11 in Region 1, 11 in Region 2, 6 in Region 3, 11 in Region 4)
- Reflective condition at R = 0
- Vacuum condition at target edge.

The cross section library used for the calculation is a combined RSIC DLC-41B/VITAMIN-C[10] and DLC-60/MACKLIB-IV,[11] coupled 25 neutron-21 gamma group library. It contains 48 isotopes with response functions and a $P_3$ Legendre expansion of the scattering cross section for each isotope. The library is based on ENDF/B-IV.

The radioactivity calculations were performed using the DKR[8] code developed at the University of Wisconsin. The code computes initial activity levels using the scalar flux distribution computed by ANISN. The main decay chains are determined and the activity is computed for selected time periods. The decay data library used by DKR is called DCDLIB[12] (Decay Chain Data Library) which contains radioactivity data from ENDF/B-IV and the Table of Isotopes.[13] The Chart of the Nuclides was relied upon when materials were not covered in ENDF/B-IV and if discrepancies were found in the Table of

TABLE 4. $S_4$ QUADRATURE SET SATISFYING EVEN MOMENT CONDITIONS (Ref. 17)

| Direction Cosine ($\mu_m$) | Weights ($\omega_m$) |
|---|---|
| -0.8688903 | 0.1666667 |
| -0.3500212 | 0.3333333 |
| 0.3500212 | 0.3333333 |
| 0.8688903 | 0.1666667 |

Isotopes. The transmutation cross sections and the decay half-lives within the DCDLIB were recently updated using the ACTL Library,[14] the Table of Isotopes, seventh edition[15] and the Chart of the Nuclides, twelfth edition.[16]

## 3. Results

All results given are for 100 MJ of released fusion energy per shot. The activation results for the Case I materials are given in Fig. 4. The very high initial activity of $3.42 \times 10^5$ curies is due to the $^6_3Li(n,p)^6_2He$ reaction. The $^6_2He$ decays by $\beta^-$ with a half-life of 810 ms thereby decaying in a very short time period. The $^8_3Li$ isotope is produced by the $(n,\gamma)$ reaction on $^7_3Li$. It also is a short-lived isotope and decays in a very short time period. The remaining isotopes shown are produced by various reactions on the Pb isotopes (see Table 3). Two radioactive isotopes are not shown in the figure. They are $^{204}_{81}Tl$ and $^{205}_{82}Pb$ with half-lives of $t_{1/2}$ = 3.77 yrs and $t_{1/2} = 1.4 \times 10^7$ yrs respectively. Their initial activities are approximately $2.93 \times 10^{-7}$ curies and $2.20 \times 10^{-9}$ curies. The $^{204}_{81}Tl$ activity will have reached a level of approximately $3 \times 10^{-15}$ curies after 100 yrs, whereas the activity level of $^{205}_{82}Pb$ remains at $2.20 \times 10^{-9}$ curies even after 1000 yrs. Thus the long term low level activity for this target is due to $^{205}_{82}Pb$. Not included in the total activity is the activity of the unburned tritium shown for comparison.

As is seen, its activity is larger than that of the remaining target materials for times less than 400 years. The resulting stable isotopes are given in Table 3.

The results of the Case II target are given in Fig. 5. Noticeable is the high initial activity of $1.13 \times 10^3$ curies due to the radioisotope $^{6}_{2}He$. $^{6}_{2}He$ and $^{9}_{3}Li$ both have very short half-lives (810 ms and 178 ms, respectively) and in less than 1 minute their contribution to the total activity is negligible. The major contributors to the total activity are the radioactive isotopes $^{186}_{73}Ta$, $^{187}_{74}W$, $^{185}_{74}W$, $^{183}_{72}Hf$ and $^{181}_{74}W$, all decaying by $\beta^-$. For the nuclear reactions which produce these radioactive isotopes and for the resulting stable isotopes see Table 3. Not shown on the figure is the low level long term activity of $^{14}_{6}C$ ($2.07 \times 10^{-14}$ curies) produced by $(n,\gamma)$ reactions on $^{13}_{6}C$ and $^{10}_{4}Be$ ($1.11 \times 10^{-13}$ curies) produced by $(n,\alpha)$ reactions on $^{12}_{6}C$ and then $(n,\gamma)$ reactions on $^{9}_{4}Be$. Noticeable again is the higher activity of the unburned tritium as compared to the total activity of the tamper material.

Figure 6 displays the results of the $CH_2$ pusher/ablator and Au tamper constituents. Once again the high initial activity of $1.13 \times 10^3$ curies is due to $^{6}_{2}He$. The short-lived isotope $^{9}_{3}Li$ is also produced with an initial activity of 18.7 curies. After approximately 3 minutes both isotopes will have decayed away. The remaining radioactive isotopes shown are from neutron interactions on $^{197}_{79}Au$ with the major contributors to the activity after approximately 2 minutes being $^{196}_{79}Au$ and $^{196m}_{79}Au$ (isomeric state of $^{196}_{79}Au$). Both are produced by a (n,2n) reaction with $^{197}_{79}Au$. $^{196}_{79}Au$ decays by electron capture and has a 6.17 day half-life. Its isomeric state, $^{196m}_{79}Au$, has a 9.7 hr half-life. The other radioactive isotope examined, $^{194}_{77}Ir$, has an activity 3 orders of magnitude lower. It decays by $\beta^-$ and has a 19.15 hr half-life. Not

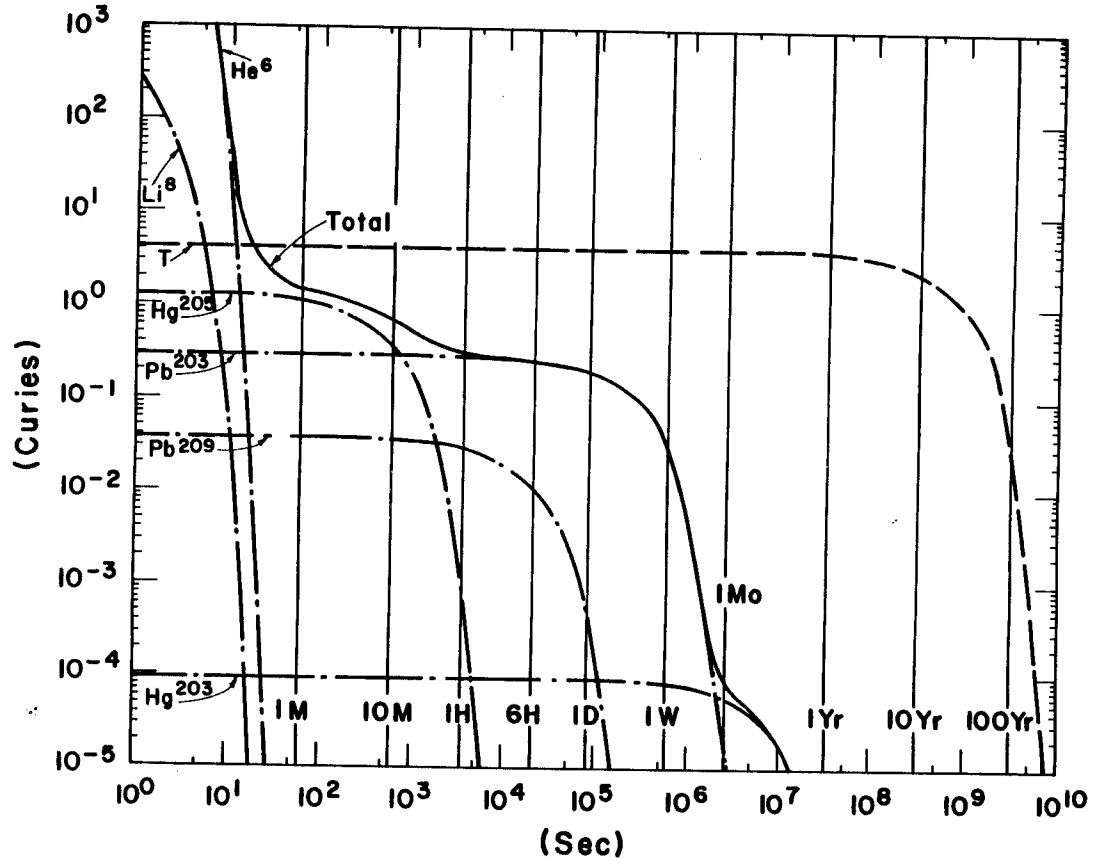


Fig. 4. Isotopic activity versus time for the Case I target constituents.

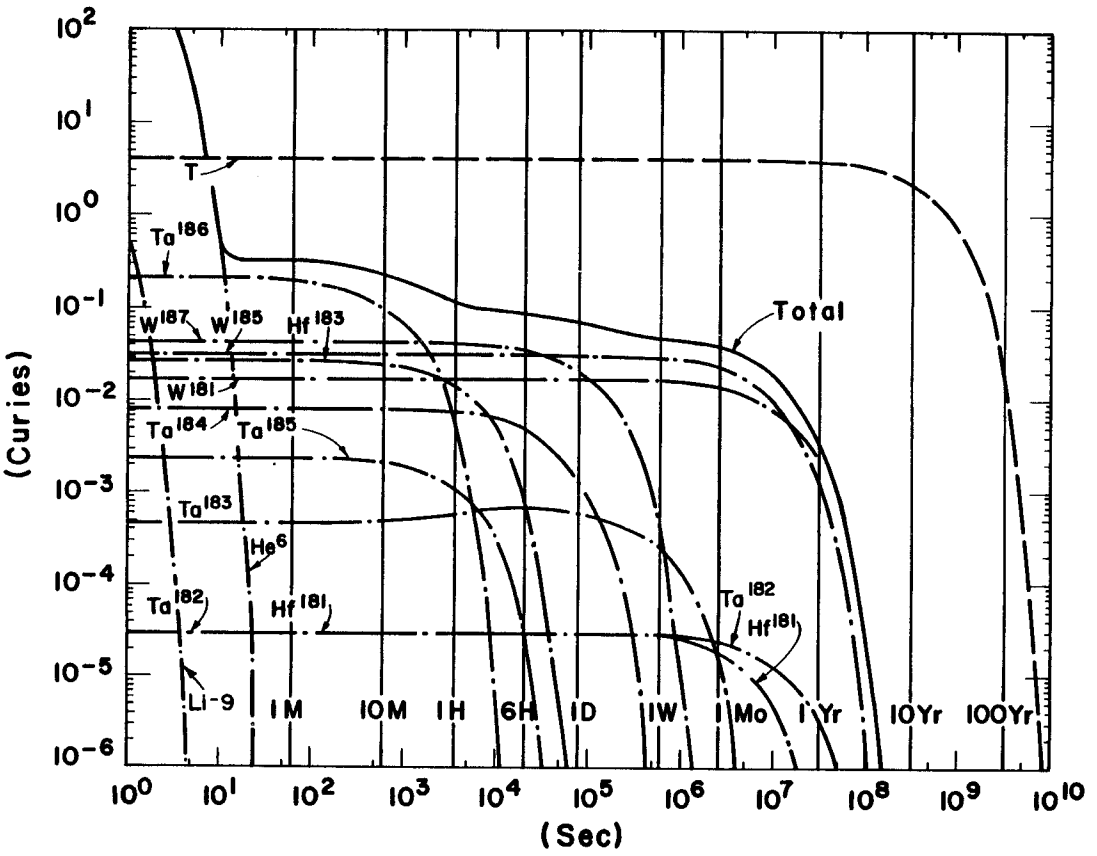


Fig. 5. Isotopic activity versus time for the Case II target constituents.

shown on the activity plot is the low level long term activity due to the $^{10}_{4}Be$ and $^{14}_{6}C$ isotopes which have initial activities of $1.11 \times 10^{-13}$ and $2.07 \times 10^{-14}$ curies, respectively. Again the unburned tritium activity is shown for comparison.

The activity results for the BeO pusher/ablator and W tamper target are shown in Fig. 7. The formation of $^{6}_{2}He$ ($t_{1/2}$ = 0.810 s) and $^{16}_{7}N$ ($t_{1/2}$ = 7.10 s) in the target lead to the very high initial activity of $6.10 \times 10^{5}$ curies which decays to the level of 0.3 curies after approximately 2 minutes. The radioactive isotopes are produced by the following reactions: $^{9}_{4}Be(n,\alpha)\ ^{6}_{2}He$ and $^{16}_{8}O(n,p)\ ^{16}_{7}N$. $^{9}_{3}Li$ is produced by a (n,p) reaction on $^{9}_{4}Be$. It has a short half-life of 178 ms and decays away in less than 1 minute. The major contributors to the total activity for times greater than 1 minute are $^{186}_{73}Ta$, $^{187}_{74}W$, $^{185}_{74}W$, $^{183}_{72}Hf$ and $^{181}_{74}W$. Not shown on the figure are the low level long term activities of $^{10}_{4}Be$ and $^{14}_{6}C$ which have initial activities of $4.86 \times 10^{-11}$ curies and $1.29 \times 10^{-15}$ curies, respectively. $^{10}_{4}Be$ has a half-life of $1.62 \times 10^{6}$ yrs and $^{14}_{6}C$ a half-life of 5734 yrs. Both decay by $\beta^{-}$. For details on the production of the radioactive isotopes and resulting stable isotopes see Table 3. Here, once again, the activity of the unburned tritium is included for comparison.

Figure 8 shows a comparison of the target activity results normalized to 1 mg of tamper material. By assuming that the activity is roughly linearly proportional to the tamper mass, one can use Fig. 8 to estimate the activity of targets with differing tamper masses. The Au tamper has a higher specific activity than the other two tamper materials. The W tamper decays somewhat slower than either the Au or Pb tampers. As seen, if only the specific

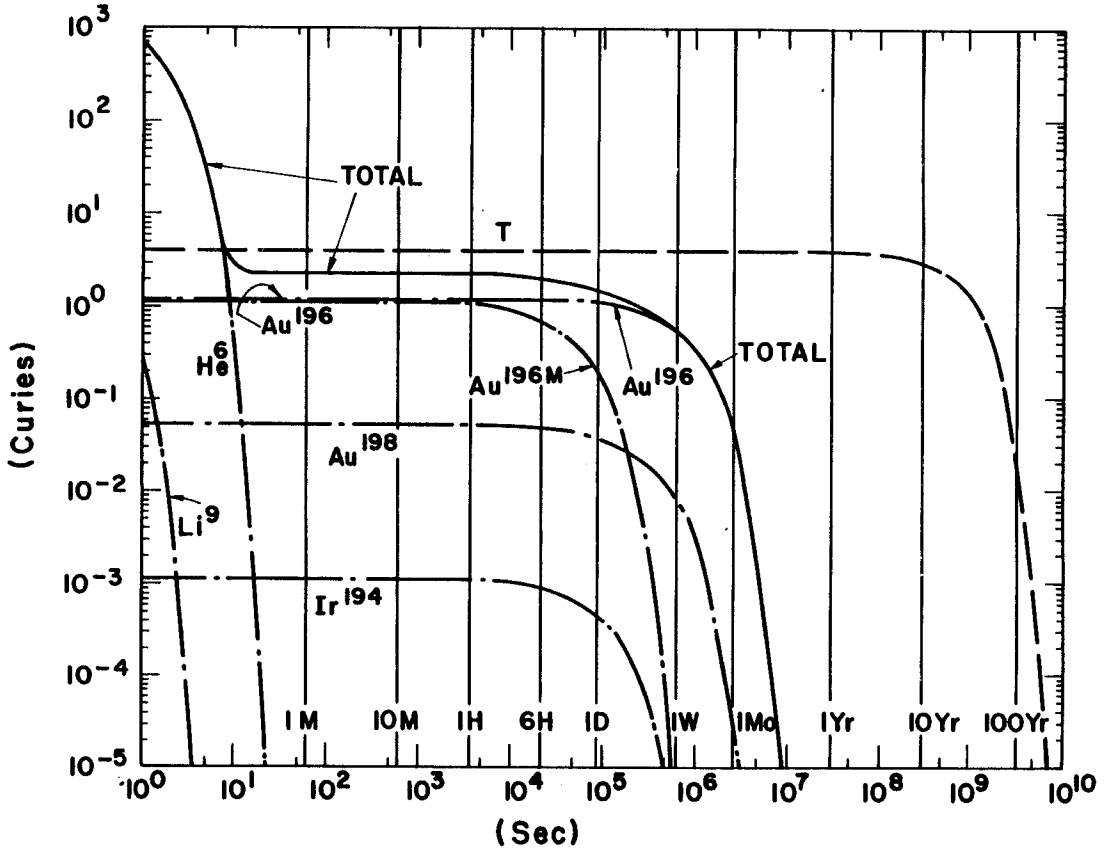


Fig. 6. Isotopic activity versus time for the Case III target constituents.

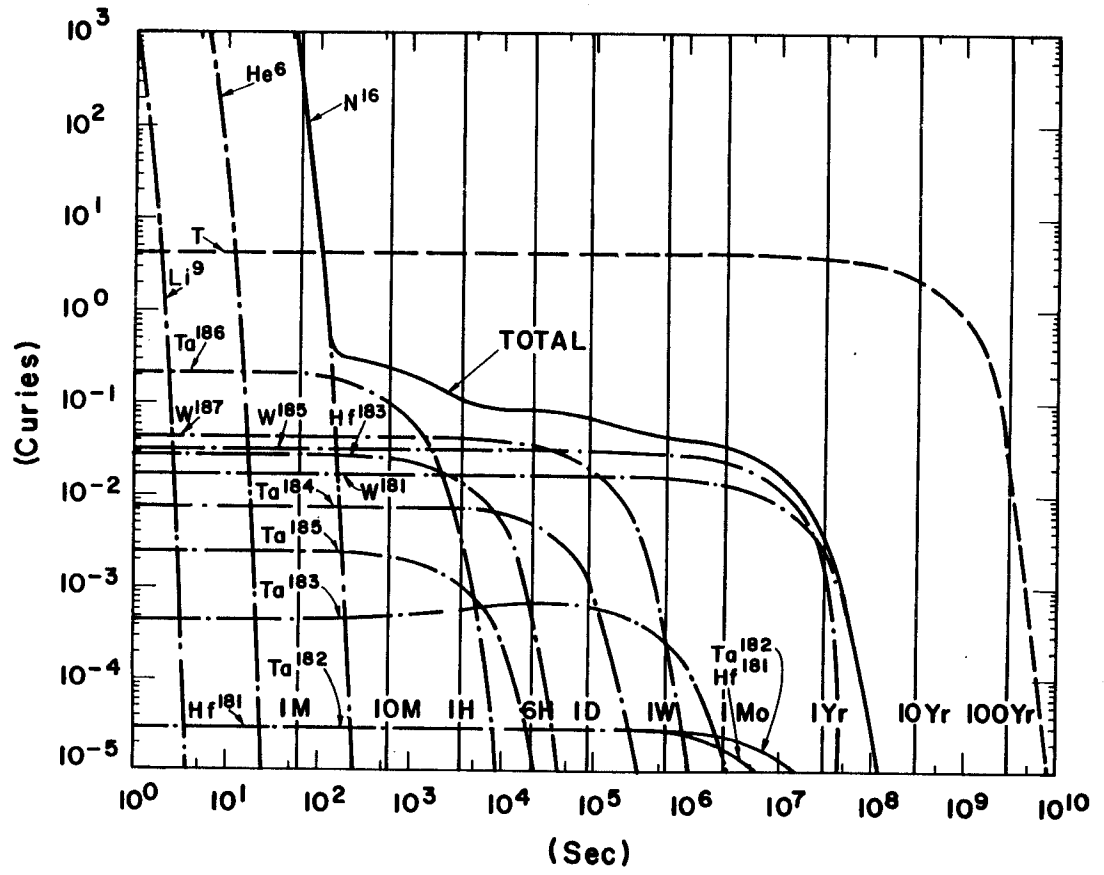


Fig. 7. Isotopic activity versus time for the Case IV target constituents.

activity is compared, the activity of the unburned tritium is 2-3 orders of magnitude higher than the activity of the tamper materials.

Several calculations were performed to determine the sensitivity of the activity results to a change in the tamper density and a change in the neutron spectrum. The tamper density was changed to its natural density value keeping the mass constant and the neutron spectrum was changed to a 14.1 MeV monoenergetic source spectrum impinging upon the pusher/ablator region's inner boundary. As can be seen from Fig. 9, the total activity of the tamper is not overly sensitive to these changes. This may be due to the fact that the moderated spectrum shown in Fig. 3 is still a very hard spectrum containing ~ 72% uncollided 14.1 MeV neutrons. A different result may be obtained if a softer source spectrum is used (containing less than 50% uncollided neutrons). The Au tamper case was used for this comparison. These calculations do not include the activity of the $^{196m}_{79}Au$ isomeric state.

## 4. Conclusions

The results have shown that all of the tamper materials have an activity within 0.3 to 2 curies on a per shot basis. If specific activity is compared, the activity of the Au tamper is somewhat higher than the other two and the W tamper takes somewhat longer to decay away. All of the pusher/ablator materials considered, $CH_2$, LiPb and BeO, have very high initial activity levels due to the production of the radioactive isotope $^{6}_{4}He$. Because of its short half-life of 810 ms, it poses no long term radioactivity problems. The long term radioactivity levels were very low on a per shot basis and are given by the following isotopes: $^{205}_{82}Pb$ activity of $2.20 \times 10^{-9}$ curies, $^{14}_{6}C$ activity of $1.83 \times 10^{-14}$ curies, and $^{10}_{4}Be$ activity of $4.86 \times 10^{-11}$ curies, all after 1000 yrs. In all cases, though, the activity of the unburned tritium exceeded that

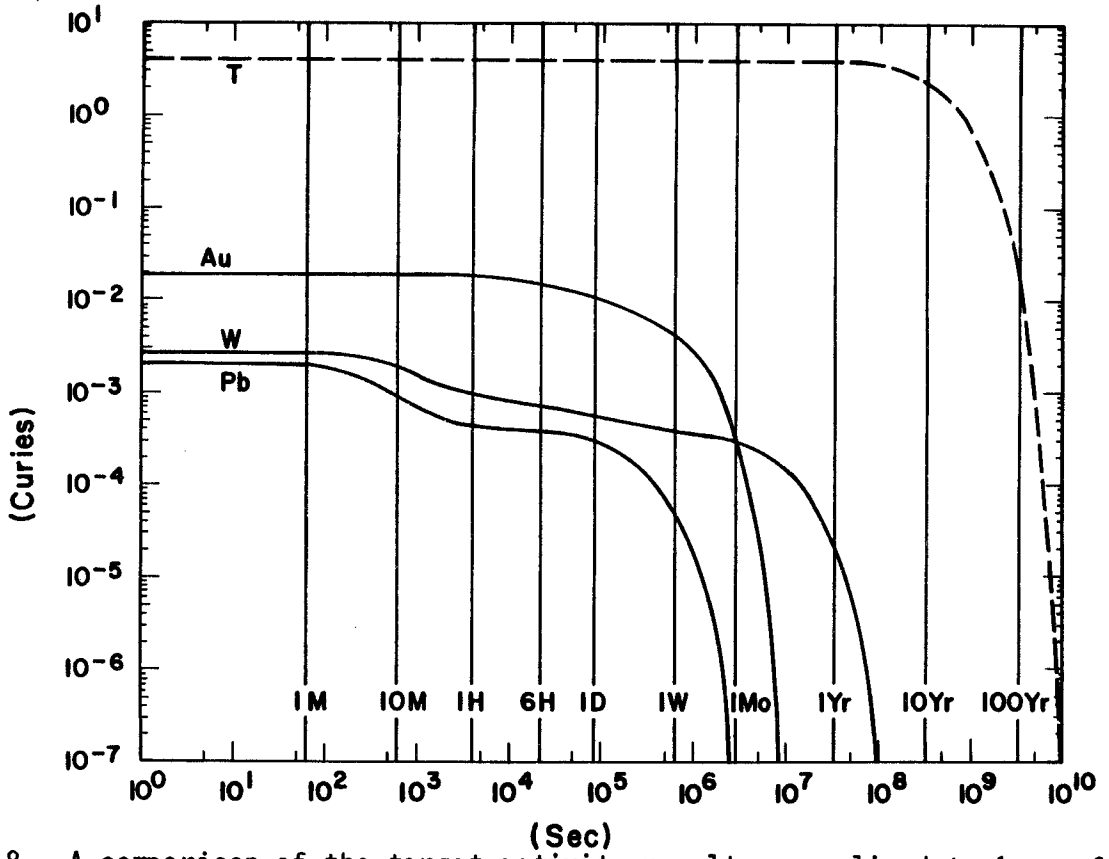


Fig. 8. A comparison of the target activity results normalized to 1 mg of tamper material.

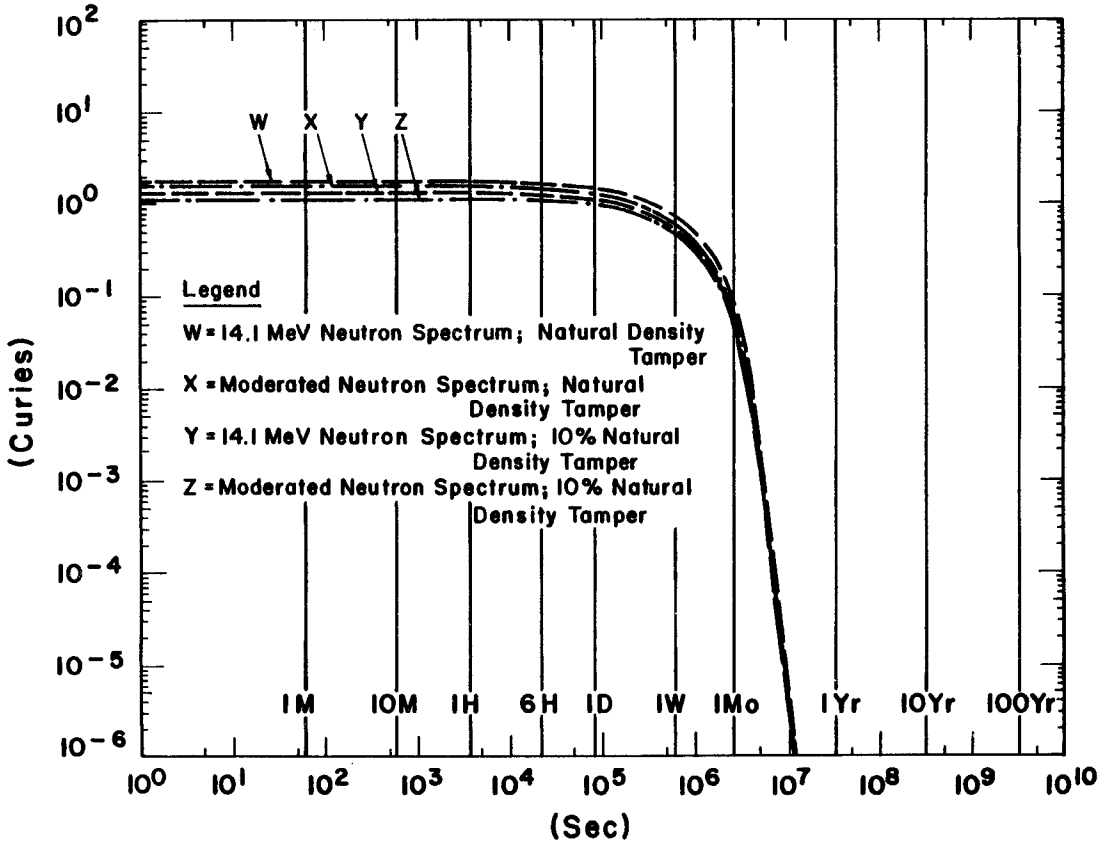


Fig. 9. Sensitivity of the activity results to a change in the tamper density and a change in the neutron spectrum.

of the target materials. This may not be as bad as it seems as the tritium will be in gaseous form and thus can be continually pumped out of the reaction chamber. The solid target materials, however, will condense and accumulate on the reaction chamber walls. It now remains to compute whether or not this accumulated activity is negligible when compared to the activity of the reactor chamber structural material. These calculations are in progress.

Acknowledgement

Support for this work has been provided by Sandia National Laboratories.

References


1. K.J. O'Brien, G.A. Moses, A.M. White, "Neutron Activation and Shielding of the Light Ion Fusion Target Development Facility," Nucl. Tech./Fusion 4, 883 (1983).

2. R.O. Bangerter, "Ion Beam Targets, Laser Program Annual Report - 1976," Lawrence Livermore Laboratory Report UCRL-50021-76, Chap. 4.

3. B. Badger et al., "HIBALL - A Conceptual Heavy Ion Beam Driven Reactor Study," University of Wisconsin Fusion Engineering Program Report UWFDM-450, KfK-3202, Parts I and II, Chap. III.

4. K.A. Long, N.A. Tahir, "Energy Deposition of Ions in Materials, and Numerical Simulations of Compression, Ignition, and Burn of Ion Beam Driven Inertial Confinement Fusion Pellets," Kernforschungszentrum Karlsruhe Report KfK-3232, Oct. 1981.

5. R. Fröhlich, B. Goel, D.L. Henderson, W. Höbel, K.A. Long and N.A. Tahir, "Heavy Ion Beam Driven Inertial Confinement Fusion Target Studies and Reactor Chamber Neutronic Analysis," Nuclear Engineering and Design 73, 201 (1982).

6. K.H. Beckurts, K. Wirtz, Nuclear Physics, Springer-Verlag, 1964.

7. F.H. Southworth, H.D. Campbell, "Neutron Downscattering in a Laser-Induced Fusioning Plasma," Nuclear Technology 32, 434 (1976).

8. Tak Yun Sung, "DKR: A Radioactivity Calculation Code for Fusion Reactors," University of Wisconsin Fusion Engineering Program Report UWFDM-170, Sept. 1976.

9. W. Engles, "A User's Manual for ANISN," RSIC Code Package CCC-254, Radiation Shielding and Information Center, Oak Ridge National Laboratory, Oak Ridge, TN.

10. RSIC Data Library Collection, "VITAMIN-C, 171 Neutron, 36 Gamma-Ray Group Cross Section Library in AMPX Interface Format for Fusion Neutronics Studies," DLC-41, ORNL.

11. RSIC Data Library Collection, "MACKLIB-IV, 171 Neutron, 36 Gamma-Ray Group Kerma Factor Library," DLC-60, ORNL.

12. T.Y. Sung and W.F. Vogelsang, "Decay Chain Data Library for Radioactivity Calculations," University of Wisconsin Fusion Engineering Program Report UWFDM-171, Sept. 1976.

13. C.M. Lederer, J.M. Hollander and I. Perlman, Table of Isotopes, Sixth Edition, Wiley, 1967.

14. M.A. Gardner and R.J. Howerton, "ACTL: Evaluated Neutron Activation Cross Section Library - Evaluation Techniques and Reaction Index," UCRL-50400, Vol. 18 (Oct. 1978).

15. C.M. Lederer, V.S. Shirley, E. Browne, et al., Table of Isotopes, Seventh Edition, Wiley, 1978.

16. Chart of the Nuclides, Twelfth Edition, General Electric Company, 1977.

17. R.D. Lathrop, B.G. Carlson, "Discrete Ordinates Angular Quadrature of the Neutron Transport Equation," Los Alamos Scientific Laboratory Report LA-3186 (1965).